Electronic Supplementary Material (ESI) for Physical Chemistry Chemical Physics.

Supplementary Material

Pushing the limits of the electrochemical window with pulse radiolysis in chloroform

Matthew J. Bird,[*,†] Andrew R. Cook,[†] Matibur Zamadar,[◦] Sadayuki Asaoka,[§] John R. Miller[*,†]

[†]Chemistry Department, Brookhaven National Laboratory, Upton, New York 11793, USA

[◦]Department of Chemistry and Biochemistry, Stephen F. Austin State University, Nacogdoches, Texas 75962-3006, USA

[§]Department of Biomolecular Engineering, Kyoto Institute of Technology, Matsugaskaki, Sakyo-ku, Kyoto 606-8585, Japan

Contents

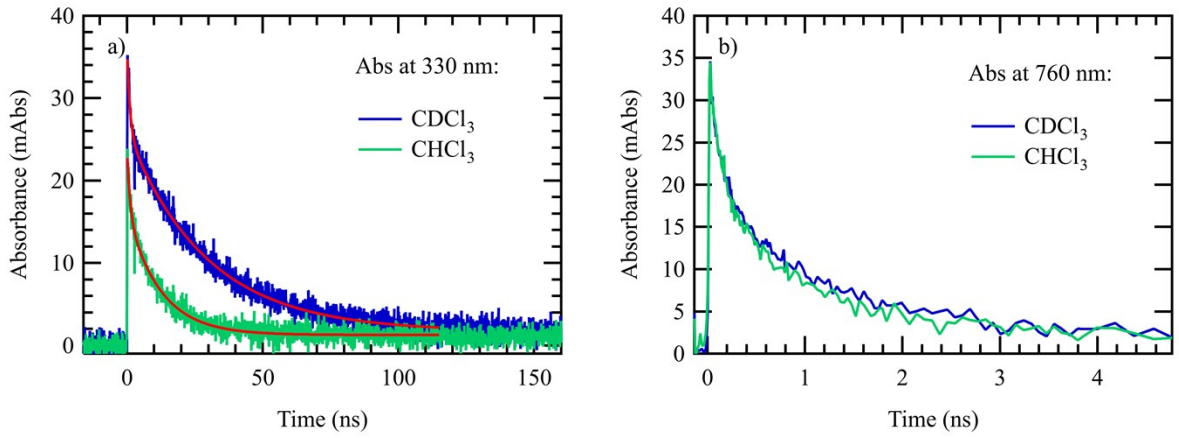

Fig S1. a) Transient absorption at 330 nm following PR in $CHCl_3$ vs $CDCl_3$ showing the decay of Cl atom. Data are fitted with the sum of two exponentials, each having a fast ~ 1 ns component. The longer-lived component has lifetimes of 12 ns and 29 ns for $CHCl_3$ and $CDCl_3$ respectively. b) Transient absorption following PR in $CHCl_3$ vs $CDCl_3$ at 760 nm comparing the kinetics of the visible absorption band.

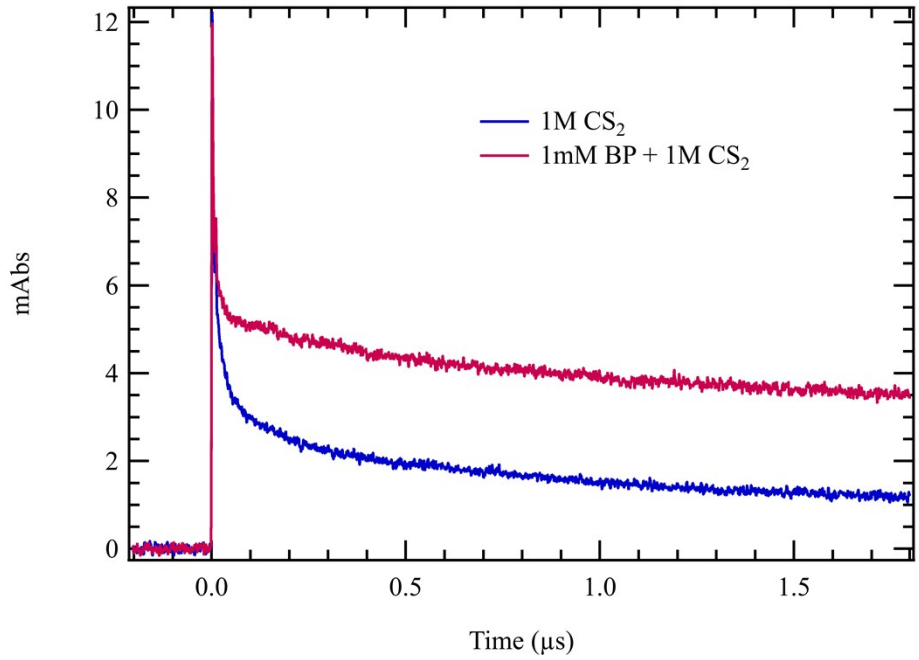

Fig S2. Transient absorption at 690 nm following PR to estimate extinction coefficient of CS_2 dimer cation by charge transfer to biphenyl. The traces are best described using a ratio of 2.0 ± 20%. The uncertainty is due to different decay rates. The reported extinction coefficient of biphenyl cation[1] of 15,550 $M^{-1}cm^{-1}$ gives CS_2 dimer cation extinction coefficient of 7,775 $M^{-1}cm^{-1}$.

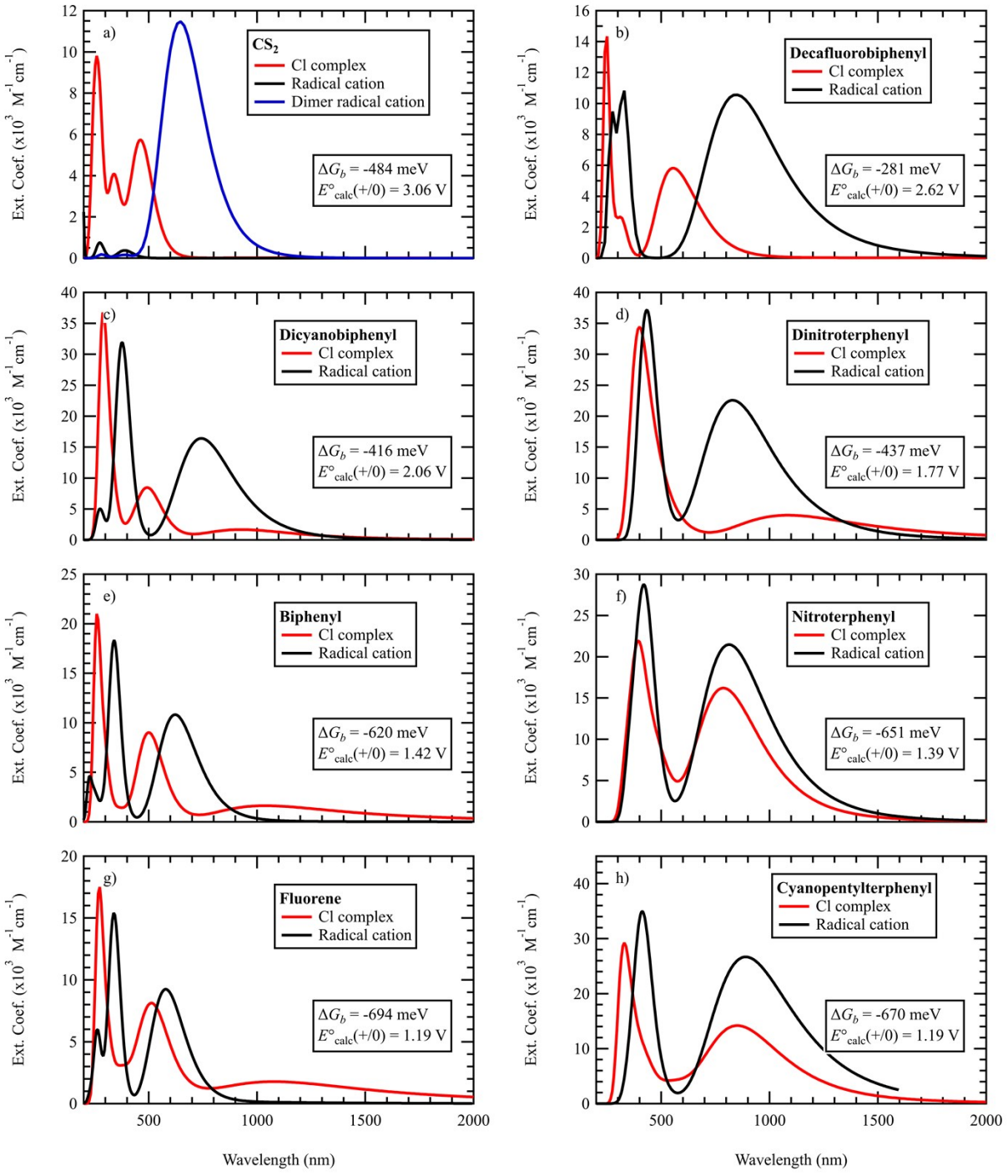

Fig S3. Calculated spectra (TD-DFT, Gaussian09[2] b3lyp/6-31+g(d) with SMD SCRF model for chloroform) for various optimized radical cations (black) and complexes with Cl atom (red). Calculated values are given for redox potentials, E°, (estimated vs Fc/Fc^{+}) and binding energies, ΔG_b, describing the standard free energy change bringing together a Cl atom with the neutral solute.

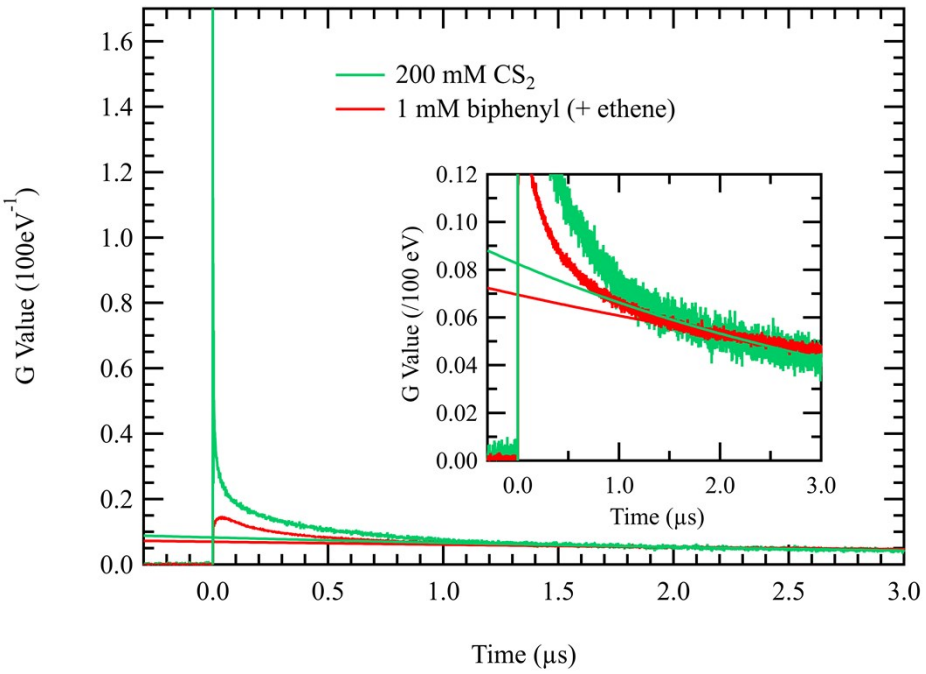

Fig S4. G-values for radical cations of CS_2 (dimer cation) and biphenyl in $CDCl_3$ obtained by extrapolating the long-lived (t >1 μs) transient absorptions to t = 0 with a single exponential using extinction coefficients of 7,775 $M^{-1}cm^{-1}$ and 15,550 $M^{-1}cm^{-1}$ respectively (from Fig S2).

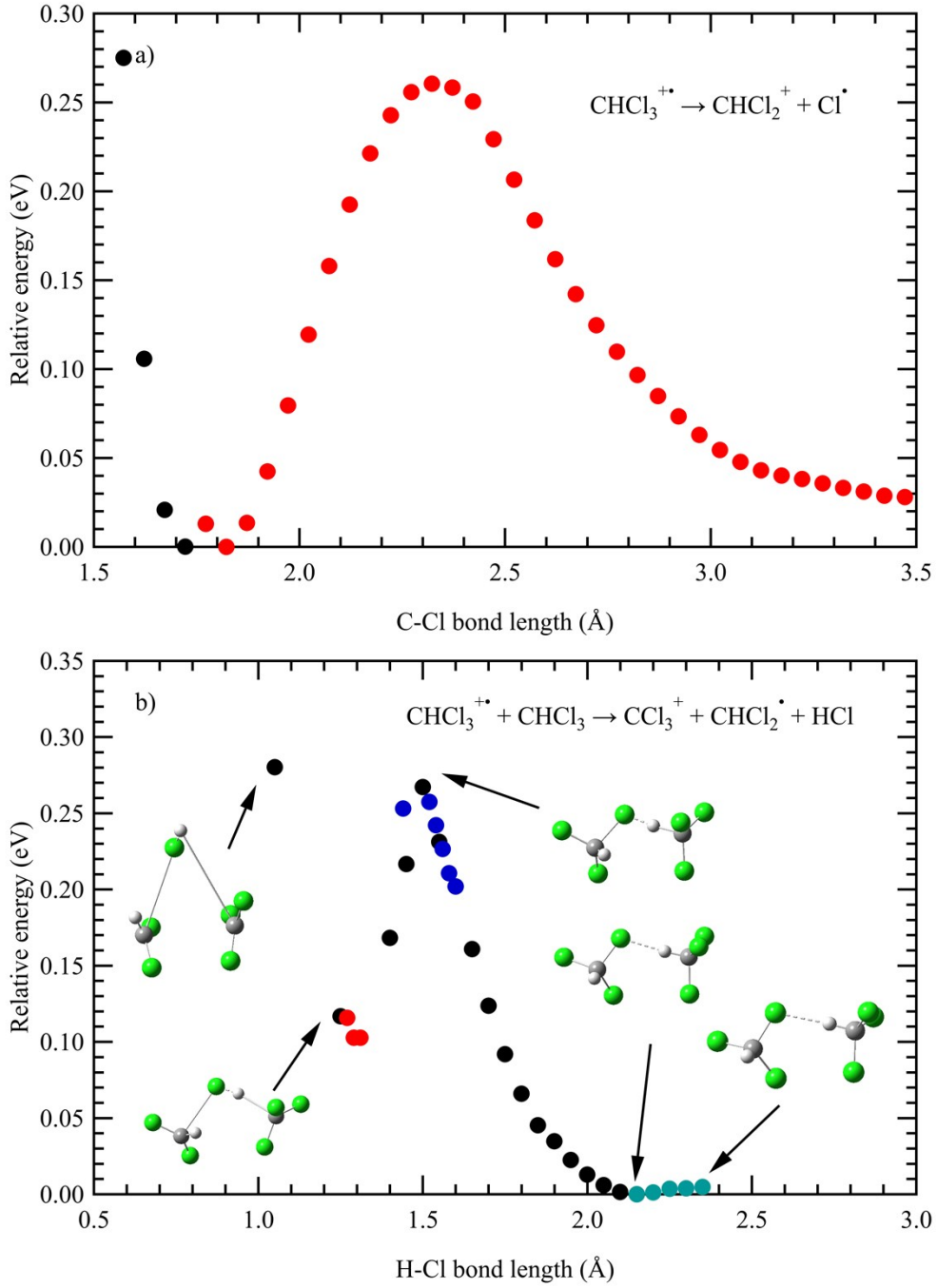

Fig S5. DFT computations (B3LYP/6-31+g* with default Gaussian09[2] solvent reaction field (SCRF) model for chloroform): a) Energy versus C-Cl bond length of chloroform radical cation during unimolecular fragmentation resulting in loss of Cl atom, relative to the energy at the optimum length of 1.77 Å b) Energy versus the H-Cl bond length in a chloroform dimer cation relative to the lowest energy point where the H-Cl bond length is 2.15 Å. The different colors are from slightly different starting conditions. Only calculations that optimized without errors are shown. The plot shows the energetic barrier for the bimolecular reaction, eqn 16, in the main text where a chloroform cation fragments in one step and HCl is one of the products. When the H-Cl bond length gets too short, the energy rises again.

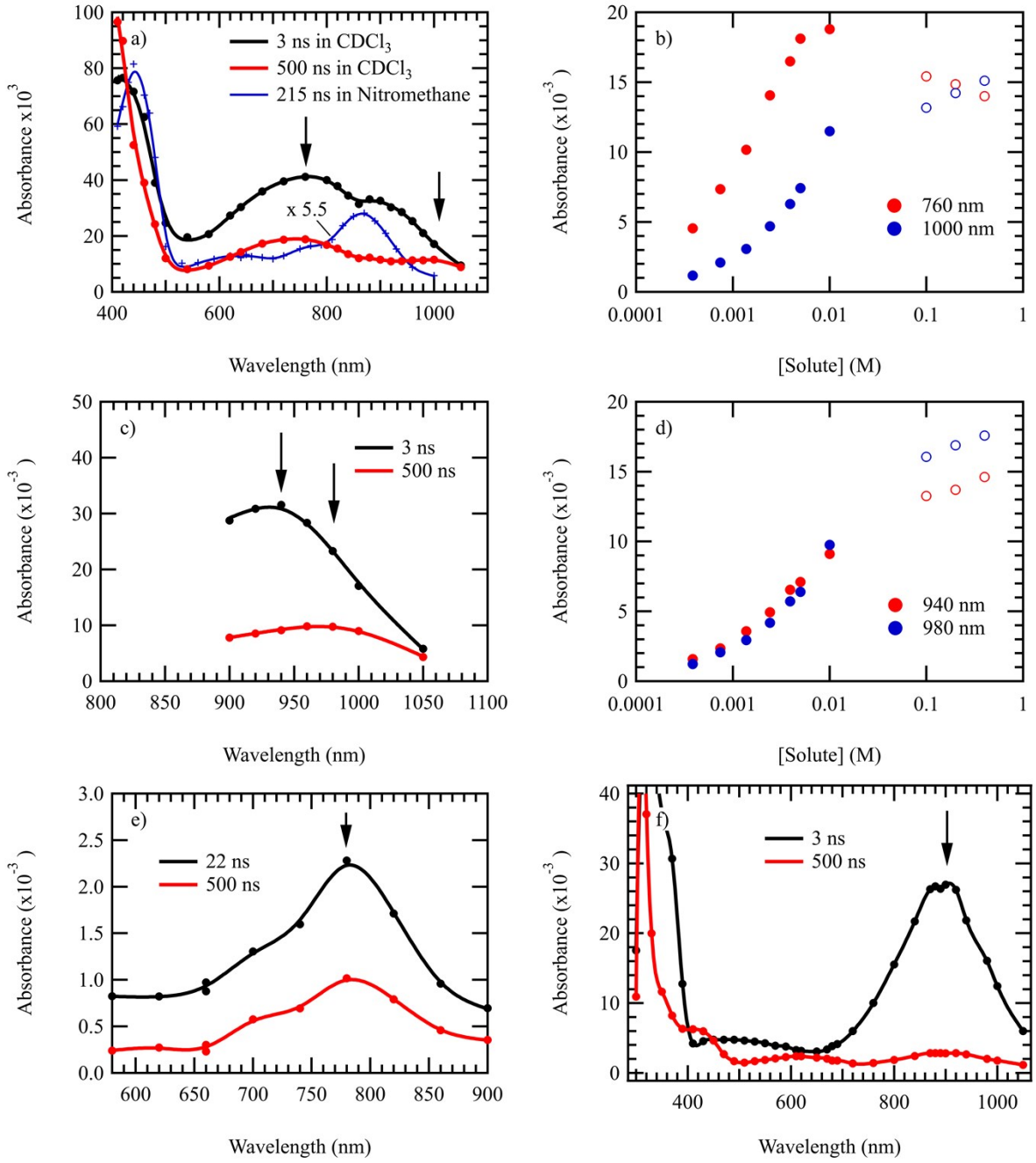

Fig S6. Spectra of various solutes used for fig 2 in the main manuscript, following pulse radiolysis in $CDCl_3$. Arrows show the wavelengths where absorption vs solute concentration at 500 ns was recorded. These spectra assess the validity of the assumption that the experiment was probing the absorption from the radical cation and not the (Cl, solute) complex. The spectra in e) and f) were taken with different concentration solutions and on a different day to those reported in fig 2. a) 10 mM 4-nitro-p-terphenyl b) 4-nitro-p-terphenyl radical cation absorption at 500 ns after pulse for various concentrations c) 10 mM 4,4''-dinitro-p-terphenyl d) 4,4''-dinitro-p-terphenyl radical cation absorption at 500 ns after pulse for various concentrations e) 1 mM 4,4'-dicyanobiphenyl and f) 50 mM decafluorobiphenyl.

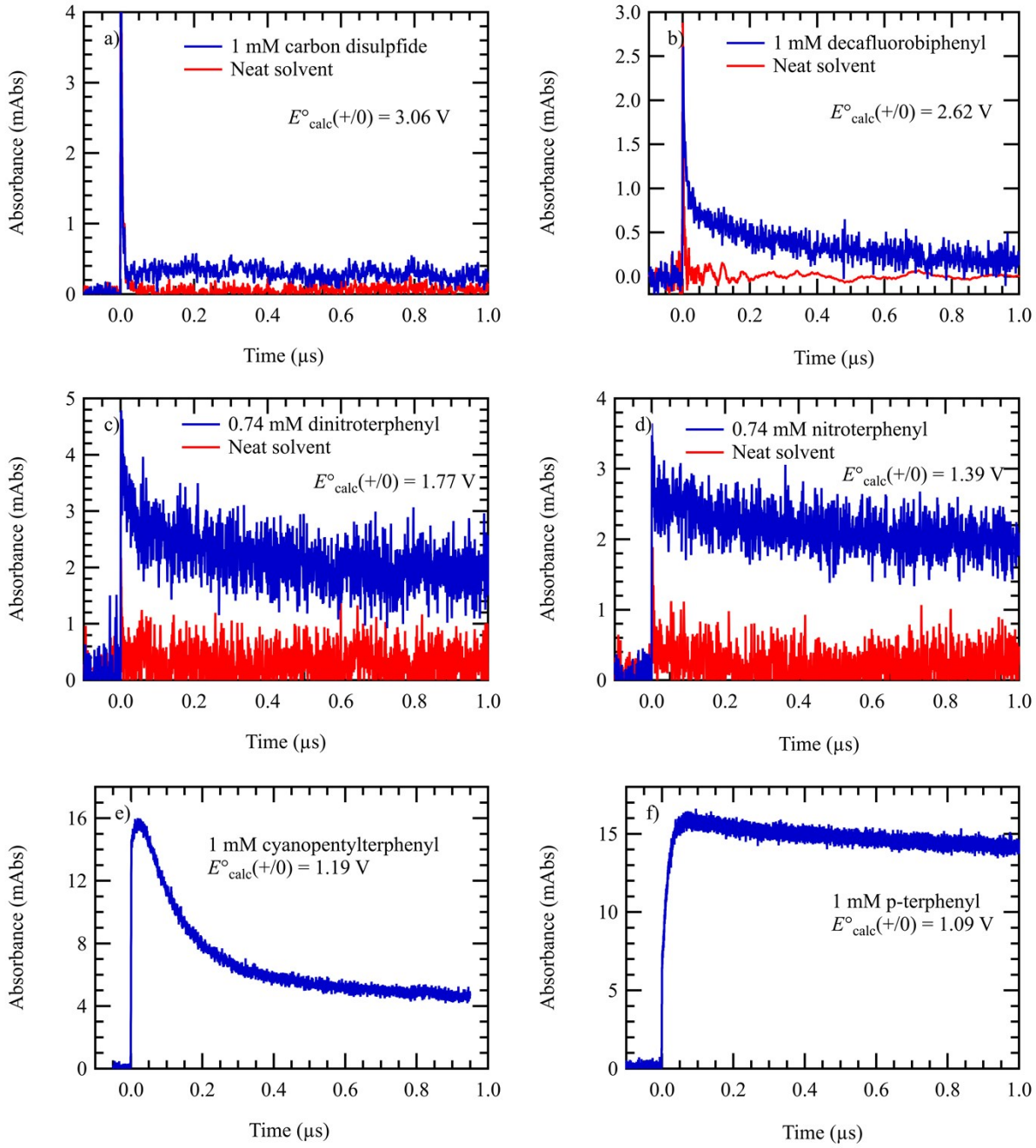

Fig S7. Transient absorption of other solutes from Table 1 following pulse radiolysis in $CDCl_3$. a) 1 mM carbon disulfide at 800 nm b) 1 mM decafluorobiphenyl at 900 nm c) 0.74 mM 4,4’’-dinitro-p-terphenyl at 980 nm d) 0.74 mM 4-nitro-p-terphenyl at 1000 nm e) 1 mM 4-cyano,4’’-pentyl-p-terphenyl at 970 nm f) 1 mM p-terphenyl at 960 nm.

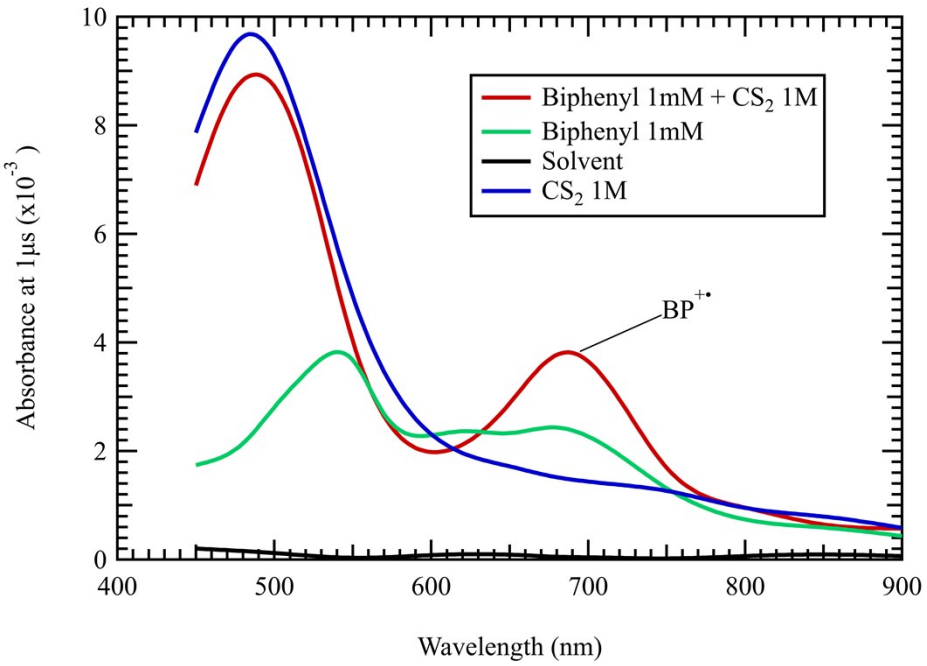

Fig S8. Spectra obtained at 1 μs following pulse radiolysis in $CDCl_3$. The biphenyl cation cannot be seen clearly in the 1 mM biphenyl solution (green trace) due to the relatively small yield of holes captured and overlapping absorptions from (BP,Cl•) complex. When CS_2 is added at 1 M to the biphenyl solution, more solvent cations are captured and transferred to the biphenyl, and the Cl atoms remain complexed with CS_2, which peaks at ~475 nm allowing the biphenyl cation to be clearly observed, peaking at 690 nm. The blue trace shows mostly (CS_2,Cl•) complex although at 1μs there is still some signs of the broad CS_2 dimer cation absorption that peaks ~690 nm.

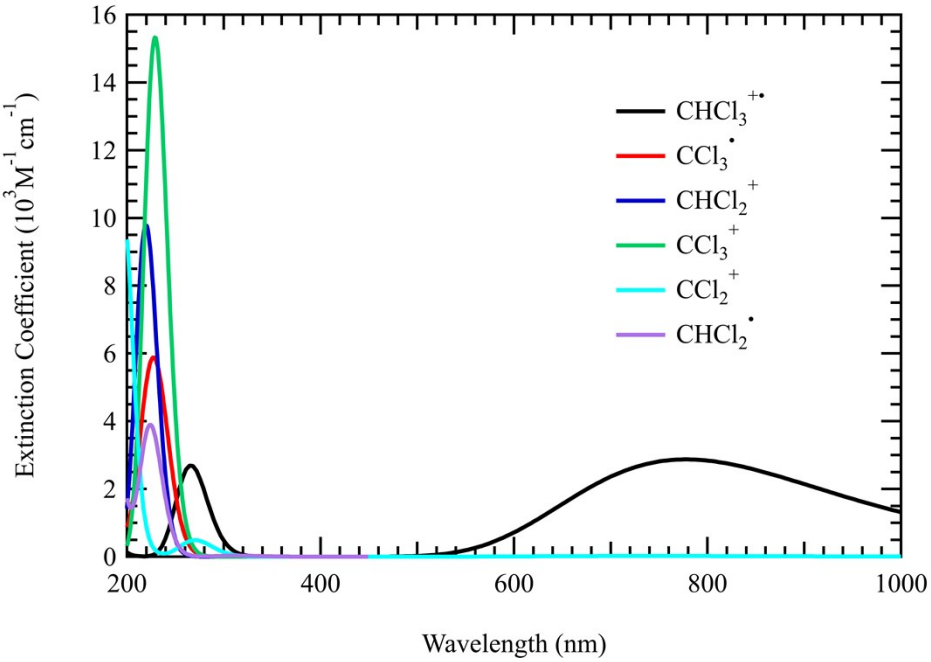

Fig S9. TD-DFT (Gaussian09[2] b3lyp/6-31+g(d) with SMD SCRF model for chloroform) estimates of the absorption spectra of various species that might be created following pulse radiolysis in liquid chloroform.

Derivation of equation 13. Hole transfer from solvent cation, A^+, to solute, B, with bimolecular rate constant, k_{att}, in competition with decay of the solvent cation through a mechanism, likely fragmentation with first order rate constant k_d. Both solvent and solute cation also assumed to decay with a common first order rate constant, k_i. This model also allows for the introduction of an impurity with the solute. The fraction of the solute that is the impurity is given by β.

$$\frac{d[A^+]}{dt} = -k_i[A^+] - k_d[A^+] - k_{att}[B][A^+] - k_{att}\beta[B][A^+]$$

$$\frac{d[B^+]}{dt} = -k_i[B^+] + k_{att}[B][A^+] - k_{att}\beta[B][B^+]$$

$$[A^+] = A_0^+ e^{(-k_i - k_d - k_{att}[B] - k_{att}\beta[B])t}$$

$$\frac{d[B^+]}{dt} = -(k_i + k_{att}\beta[B])[B^+] + k_{att}[B]A_0^+ e^{(-k_i - k_d - k_{att}[B] - k_{att}\beta[B])t}$$

Using the chain rule, we can obtain:

$$\int \frac{d[B^+]e^{(k_i + k_{att}\beta[B])t}}{dt} dt = \int e^{k_i(k_i + k_{att}\beta[B])t} k_{att}[B]A_0^+ e^{(-k_i - k_d - k_{att}[B] - k_{att}\beta[B])t} dt$$

$$[B^+]e^{(k_i + k_{att}\beta[B])t} = \int k_{att}[B]A_0^+ e^{(-k_d - k_{att}[B])t} dt$$

$$[B^+]e^{(k_i + k_{att}\beta[B])t} = \frac{k_{att}[B]A_0^+ e^{(-k_d - k_{att}[B])t}}{-k_d - k_{att}[B]} + C$$

At t=0, $[B^+] = 0$

$$[B^+] = \frac{k_{att}[B]A_0^+}{k_d + k_{att}[B]}\left(1 - e^{(-k_d - k_{att}[B])t}\right)e^{-(k_i + k_{att}\beta[B])t}$$

for $[B]$ big, and impurities small:

$$[B^+]_{max} = A_0^+ e^{-k_i t}$$

Ratio of $[B^+]$ to $[B^+]_{max}$:

$$\frac{[B^+]}{[B^+]_{max}} = \frac{k_{att}[B]}{k_d + k_{att}[B]}\left(1 - e^{(-k_d - k_{att}[B])t}\right)e^{-k_{att}\beta[B]t}$$

Converting to absorbance:

$$\frac{Abs(B^+)}{Abs(B^+)_{max}} = \frac{k_{att}[B]}{k_d + k_{att}[B]}\left(1 - e^{(-k_d - k_{att}[B])t}\right)e^{-k_{att}\beta[B]t}$$

References

1. A. R. Cook, M. J. Bird, S. Asaoka and J. R. Miller, *J. Phys. Chem. A*, 2013, **117**, 7712-7720.
2. M. J. Frisch, G. W. Trucks, H. B. Schlegel, G. E. Scuseria, M. A. Robb, J. R. Cheeseman, G. Scalmani, V. Barone, B. Mennucci, G. A. Petersson, H. Nakatsuji, M. Caricato, X. Li, H. P. Hratchian, A. F. Izmaylov, J. Bloino, G. Zheng, J. L. Sonnenberg, M. Hada, M. Ehara, K. Toyota, R. Fukuda, J. Hasegawa, M. Ishida, T. Nakajima, Y. Honda, O. Kitao, H. Nakai, T. Vreven, J. A. Montgomery, Jr., J. E. Peralta, F. Ogliaro, M. Bearpark, J. J. Heyd, E. Brothers, K. N. Kudin, V. N. Staroverov, R. Kobayashi, J. Normand, K. Raghavachari, A. Rendell, J. C. Burant, S. S. Iyengar, J. Tomasi, M. Cossi, N. Rega, N. J. Millam, M. Klene, J. E. Knox, J. B. Cross, V. Bakken, C. Adamo, J. Jaramillo, R. Gomperts, R. E. Stratmann, O. Yazyev, A. J. Austin, R. Cammi, C. Pomelli, J. W. Ochterski, R. L. Martin, K. Morokuma, V. G. Zakrzewski, G. A. Voth, P. Salvador, J. J. Dannenberg, S. Dapprich, A. D. Daniels, Ö. Farkas, J. B. Foresman, J. V. Ortiz, J. Cioslowski and D. J. Fox, Gaussian, Inc., Wallingford CT2009, vol. Revision D.01.